SIMPLEVLA-RL: SCALING VLA TRAINING VIA RE-INFORCEMENT LEARNING

Anonymous authors

000

001

002003004

006 007 008

009 010

011

012

013

014

015

016

017

018

019

021

023

024

025

026

027

028

031

033 034

038

039 040

041

042

043 044

045

047

048

051

052

Paper under double-blind review

ABSTRACT

Vision-Language-Action (VLA) models have emerged as a powerful paradigm for robotic manipulation. Despite substantial progress enabled by large-scale pretraining and supervised fine-tuning (SFT), these models face two fundamental challenges: (i) the scarcity and high cost of large-scale robotic trajectories required for SFT scaling, and (ii) limited generalization to tasks under distribution shift. To overcome these limitations, we explore reinforcement learning (RL) as a pathway to scaling VLA training beyond limited datasets. Inspired by LLM breakthroughs where RL with outcome rewards enhances step-by-step reasoning, we ask: *Can* outcome-driven RL improve long-horizon step-by-step action planning of VLA? In this work, we introduce **SimpleVLA-RL**, an efficient RL framework tailored for VLA models. Building upon veRL, we introduce VLA-specific trajectory sampling, scalable parallelization, multi-environment rendering, and optimized loss computation. Applied to OpenVLA-OFT, SimpleVLA-RL achieves 99% of SoTA performance on LIBERO and 80% relative improvement on RoboTwin 1.0&2.0, outperforming π_0 with our proposed exploration-enhancing strategies. **SimpleVLA-RL** reduces dependence on large-scale data, enables robust generalization, and remarkably surpasses SFT in real-world tasks. Moreover, we identify a novel phenomenon "pushcut" during RL training, wherein the policy discovers unseen patterns beyond those seen in previous training process.

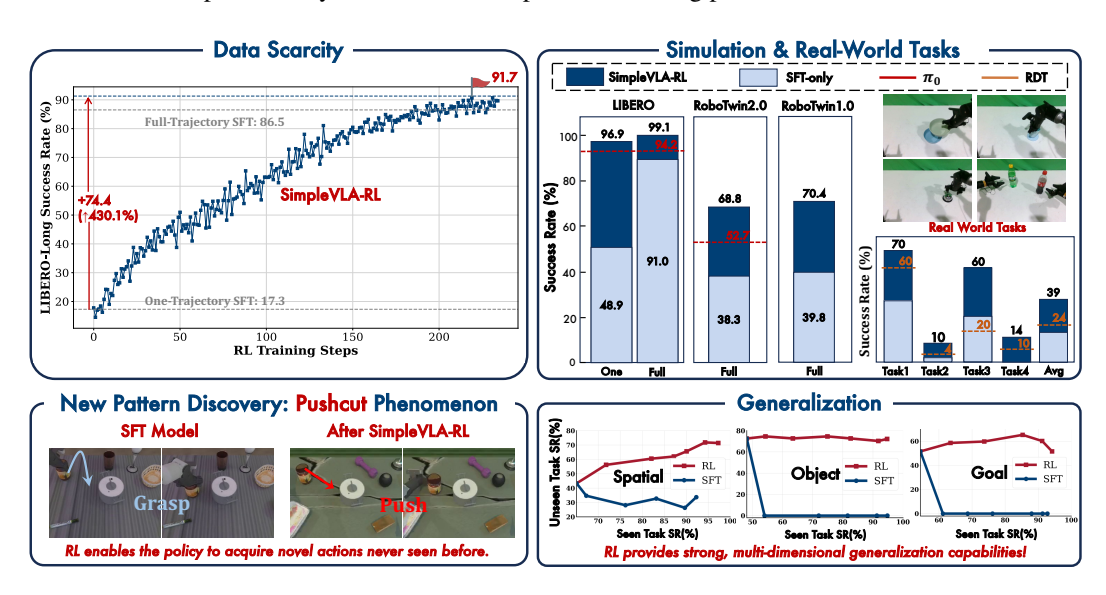


Figure 1: Overview of **SimpleVLA-RL**. An efficient RL framework for VLA that improves long-horizon planning under data scarcity, outperforms SFT in simulation and real-world tasks, reveals a "pushcut" new-action phenomenon, and strengthens spatial/object/goal generalization.

1 Introduction

Vision-Language-Action (VLA) models have emerged as a promising approach for general robotic manipulation by integrating visual perception, language understanding, and action generation in a unified framework (Firoozi et al., 2025; Kim et al., 2024; Zhong et al., 2025). Current VLA training

paradigm consists of two stages: large-scale pretraining on multimodal data (human manipulation videos (Sapkota et al., 2025), image-text pairs, and heterogeneous robot datasets (O'Neill et al., 2024)), followed by supervised fine-tuning (SFT) on additional high-quality robot trajectories to enhance task-specific capabilities.

While imitation learning paradigm has achieved notable progress (Intelligence et al., 2025), its heavy dependence on large-scale, high-quality data poses a fundamental bottleneck that constrains further development of VLA models: the Generalization Bottleneck from Data Scarcity (Schulman et al., 2017b). 1) Data Scarcity: Scaling VLA training through SFT requires massive amounts of high-quality robot trajectories, yet such data remains scarce and prohibitively expensive (Gao et al., 2024). Collecting expert demonstrations demands carefully designed scenarios, diverse manipulation objects, and skilled operators, which severely constrains both data scale and diversity (Bu et al., 2025a; Team et al., 2025a). 2) Poor Generalization: This data scarcity leads to a fundamental mismatch between training distributions and open-ended real-world tasks (Liu et al., 2025a). VLA models trained on limited, scene-specific data tend to memorize patterns rather than learn generalizable skills. Consequently, even minor distribution shifts, unseen objects or environments, can cause compounding errors that severely limit generalization (Ross & Bagnell, 2010). This problem becomes especially critical in compositional and long-horizon tasks (Gupta et al., 2019), revealing that simply scaling SFT data cannot build generalizable VLA models to the open world.

To overcome this generalization bottleneck, VLA models need a learning mechanism capable of interactive refinement beyond limited static datasets. Reinforcement Learning (RL) offers this capability through trial-and-error environmental interaction (Xu et al., 2024). However, traditional robotics RL requires hand-crafted reward functions for each task, limiting scalability and generalization to novel scenarios where rewards are undefined (Ibarz et al., 2021; Kroemer et al., 2021; Ma et al., 2023). This creates a dilemma: SFT is constrained by data, while traditional RL is constrained by reward engineering. Recent breakthroughs in Large Reasoning Models (LRMs) provide a crucial insight: using only sparse outcome rewards, RL can significantly enhance models' ability to generate correct step-by-step reasoning chains (Guo et al., 2025a; Yang et al., 2025; Zeng et al., 2025; Team et al., 2025b). This raises a critical question for VLAs: Can we leverage this outcomedriven RL paradigm to enhance VLA models' ability to generate step-by-step correct actions? However, applying RL to VLA models presents unique technical challenges. First, unlike open-loop text generation in LLMs, VLAs require closed-loop environment interaction with continuous visual feedback, creating substantial computational overhead (Wang et al., 2025). Second, manipulation tasks face inefficient exploration due to high-dimensional action spaces and sparse rewards (Zhou et al., 2025). Third, existing RL frameworks lack VLA-specific infrastructure for efficient inference and parallel environment interaction (Luo et al., 2025).

We introduce **SimpleVLA-RL**, an effective RL framework for VLA models. Building upon Volcano Engine Reinforcement Learning for LLMs (veRL) (Sheng et al., 2024), we enable end-to-end rule-based online RL for VLA models through VLA-specific interactive trajectory sampling and loss computation. To support scalable RL training, we extend veRL with parallel multi-environment rendering and adapt it into a unified training–inference–rendering framework. We also design three exploration-enhancing strategies. Through **SimpleVLA-RL**, we significantly improve VLA performance under data-scarce conditions, enhance generalization capabilities, and achieve noticeable gains in real-world applications. Surprisingly, during RL training, the policy discovers novel patterns beyond those in supervised data, a phenomenon we term "pushcut". Our contributions include:

- Efficient online RL framework for VLA: We develop an efficient end-to-end VLA online RL framework based on veRL that enables stable, sample-efficient training, optimized for rendering parallelization and distributed training & inference.
- SOTA performance: We incorporate exploration-enhancing strategies, yielding consistent performance improvements of 10–15%. Moreover, SimpleVLA-RL surpasses multiple SoTA baselines on both LIBERO and RoboTwin 1.0 & 2.0.
- Data efficiency and generalization: With only a single demonstration per task, RL boosts LIBERO-Long success rates from 17.1% to 91.7%, and significantly outperforms SFT in spatial, object, and task generalization.
- Real-world deployment capability: Simulation-trained policies transfer effectively to real-world, achieving strong sim-to-real improvements without requiring real robot data.

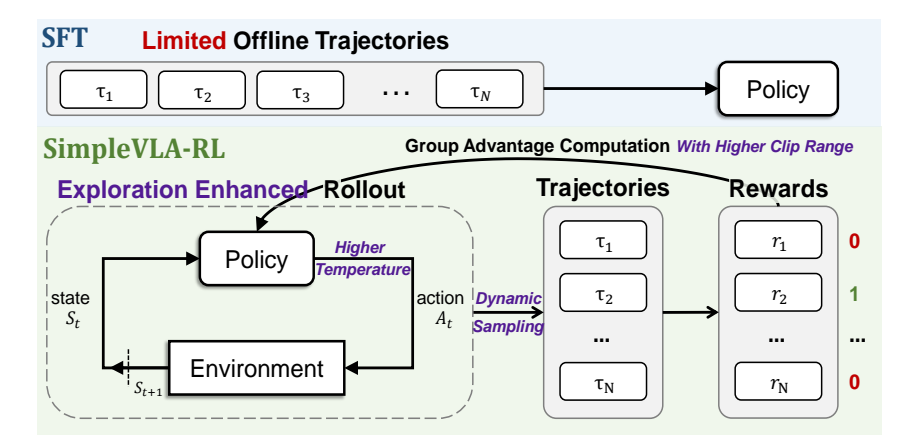


Figure 2: Overview of SimpleVLA-RL.

2 SIMPLEVLA-RL

DeepSeek-R1 (Guo et al., 2025a) has achieved remarkable performance gains through online RL with the simple, scalable rule-based reward, highlighting a promising training paradigm. In this section, we introduce **SimpleVLA-RL**, which extends this rule-based online RL framework to VLA models for embodied manipulation tasks as shown in Figure 2. Specifically, our training framework proceeds as follows: we begin by generating multiple trajectories for each input via random sampling (§2.1). Each trajectory is then assigned a simple outcome reward (1 for success, 0 for failure) based on environment feedback (§ 2.2). Leveraging these rewards together with the corresponding action token probabilities, we compute the GRPO loss to update the policy model (§ 2.4).

2.1 Interactive VLA Rollout

RL on VLA models differs fundamentally from LLMs in trajectory generation. To enable online RL, policy models need to generate diverse trajectories from an input for effective exploration. While LLMs naturally achieve this diversity through random sampling on text token distributions (Renze, 2024; De Rosa & Papa, 2021), VLA models face a unique challenge due to their action decoding strategies. Current VLA models often employ three strategies: (1) generating action token distributions similar to LLMs (Black et al., 2024; Kim et al., 2024), (2) diffusion-based denoising on latent states (Liu et al., 2024; Cheang et al., 2025), and (3) deterministic regression via MLPs (Kim et al., 2025). Among these, the token-based approach is most compatible with PPO-like RL algorithms, as it naturally provides action distributions necessary for both random sampling and policy gradient computation. Therefore, we adopt this approach, where the VLA model outputs action token probability distributions and employs random sampling to generate diverse trajectories.

Furthermore, for a given input query, LLM rollout proceeds by autoregressively generating tokens until reaching a stop token or max output length. In contrast, VLA rollout requires continuous interaction with the environment to update the visual observation and robot state dynamically (as detailed in Appendix B). This closed-loop interaction is necessary because each robotic action alters the environment, and subsequent actions must be conditioned on real-time sensory feedback. We present the comparison of the rollout algorithm pseudo-code of LLMs and VLA in Listing 1.

2.2 OUTCOME REWARD MODELING

SimpleVLA-RL employs a straightforward binary reward function for RL training. Unlike traditional RL approaches that require carefully crafted reward functions (Hadfield-Menell et al., 2017; Knox et al., 2023; Booth et al., 2023), we follow DeepSeek-R1's approach by assigning trajectory-level rewards of either 0 or 1 based solely on task completion. When the VLA model successfully completes a task, the entire trajectory is assigned a reward of 1; otherwise, it receives a reward of 0. For gradient computation, these trajectory-level rewards are uniformly propagated to the individual action tokens. Consequently, all tokens within successful trajectories are assigned a reward of 1, whereas those in unsuccessful trajectories are assigned a reward function is:

$$R(a_{i,t} \mid s_{i,t}) = \begin{cases} 1, & \text{is_successful[traj}_i(a_i, s_i)], \\ 0, & \text{otherwise.} \end{cases}$$
 (1)

This simple outcome-level reward is simple yet effective: scalable, broadly applicable across environments, and free from complex process-based design (Wu et al., 2021). By focusing solely on task completion, it avoids the non-transferability issues typical of task-specific rewards.

2.3 EXPLORATION ENHANCEMENTS

Previous works (Yu et al., 2025; Liu et al., 2025b;d; An et al., 2025) have demonstrated that encouraging exploration during RL is critical. We observe that this factor becomes even more crucial in VLA RL. Manipulation tasks typically allow for a wide range of valid solutions. However, VLA models tend to converge on a narrow set of solution patterns, largely due to the homogeneity of their training trajectories, which limits the efficiency of RL. Promoting exploration encourages models to discover novel strategies and broaden the solution space, a property that is particularly advantageous in scenarios with low success rates. Building on this insight, we implement three key modifications to enhance the exploration of RL training: 1) employing dynamic sampling during trajectory rollout, 2) adjusting the clip range in the GRPO training objective, 3) and increasing the sampling temperature during rollout.

Dynamic Sampling Critic-free RL algorithms suffer from vanishing gradients when trajectories are assigned the same rewards. For example, GRPO computes advantages using group-relative normalization, comparing each response's reward to the mean and standard deviation of rewards within its group of sampled outputs. When all trajectories share identical rewards, their advantage estimation becomes zero, resulting in null gradients and causing unstable training dynamics.

We address this challenge through Dynamic Sampling (Yu et al., 2025; Cui et al., 2025a), a method that has been proven effective in LLM RL (Cui et al., 2025a; Yu et al., 2025; Team et al., 2025b; Shi et al., 2025). During rollout, we exclude groups in which all trajectories either succeed or fail. Sampling proceeds until the batch consists solely of groups with mixed outcomes, which can be formally expressed as:

$$0 < |\{\operatorname{traj}_{i}(a_{i}, s_{i}) \mid \operatorname{is_successful}[\operatorname{traj}_{i}(a_{i}, s_{i})]\}| < G. \tag{2}$$

This ensures non-zero advantage estimates and stable gradient flow throughout training.

Clipping Higher PPO and GRPO employ clipping over the importance sampling ratio to restrict the trust region (Schulman et al., 2015) and enhance RL stability (Schulman et al., 2017a; Shao et al., 2024). However, the upper clipping threshold restricts the probability increase of low-probability tokens, thereby potentially constraining exploration. Following DAPO (Yu et al., 2025), we modify the clipping range in the GRPO training objective from [0.8, 1.2] to [0.8, 1.28].

Higher Rollout Temperature Recent works on LLM RL adjusting the rollout temperature to promote exploration have been widely shown to be effective, with sampling at higher temperatures yielding particularly notable improvements (An et al., 2025; Liu et al., 2025d; Liao et al., 2025). To encourage the VLA model to generate more diverse trajectories during the rollout phase, we increase the sampling temperature from 1.0 to 1.6. As shown in Figure 3, these modifications led to notable improvements.

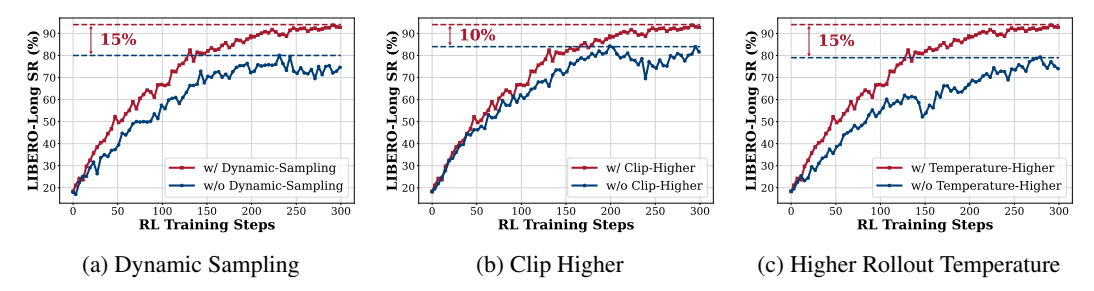


Figure 3: The effectiveness of three key enhancements: dynamic sampling, higher rollout temperature, and clip higher.

2.4 Training Objective

We use the adopted GRPO algorithm (Shao et al., 2024) for online RL training on VLA models, with modifications as introduced in Section 2.3. Moreover, we remove the KL divergence regularization

following DAPO (Yu et al., 2025). This eliminates the need for a reference model during training, reducing memory consumption and accelerating the training. Additionally, the KL penalty constrains policy divergence from a fixed reference, potentially limiting exploration of new behaviors. Therefore, the policy is optimized via the following objective:

$$\mathcal{J}(\theta) \!=\! \mathbb{E}_{s_0 \sim \mathcal{D}, \{a_t\}_{i=1}^G \sim \pi_{\theta_{\text{old}}}(\cdot \mid s_t)} \left[\frac{1}{G} \sum_{i=1}^G \frac{1}{|a_i|} \sum_{t=1}^{|a_i|} \min \left(r_{i,t}(\theta) \hat{A}_i, \, \operatorname{clip}\left(r_{i,t}(\theta), 1 - \varepsilon_L, 1 + \varepsilon_H \right) \hat{A}_i \right) \right]$$

s.t.
$$0 < |\{\operatorname{traj}_i(a_i, s_i) : \operatorname{success}[\operatorname{traj}_i(a_i, s_i)]\}| < G,$$
(3)

where

$$r_{i,t}(\theta) = \frac{\pi_{\theta}(a_{i,t} \mid s_{i,t})}{\pi_{\theta_{\text{old}}}(a_{i,t} \mid s_{i,t})}, \quad \hat{A}_i = \frac{R_i - \text{mean}(\{R_i\}_{i=1}^G)}{\text{std}(\{R_i\}_{i=1}^G)}. \tag{4}$$

Table 1: Main results of different VLA models on RoboTwin1.0.

Model	RoboTwin1.0						
1,10401	Hammer Beat	Block Handover	Blocks Stack	Shoe Place	Avg		
DP	0.0	12.0	7.1	4.3	5.9		
DP3	64.7	84.3	24.0	59.3	58.1		
OpenVLA-OFT w/ ours Δ	67.2	61.6	7.1	23.4	39.8		
	92.6	89.6	40.2	59.3	70.4		
	+25.4	+28.0	+33.1	+35.9	+30.6		

3 EXPERIMENTS

3.1 Experimental Setup

Benchmarks We evaluate SimpleVLA-RL on three simulation benchmarks—LIBERO (Liu et al., 2023), RoboTwin1.0 (Mu et al., 2025), and RoboTwin2.0 (Chen et al., 2025a), and conduct real-world experiments on RoboTwin2.0 tasks. LIBERO is a language-guided manipulation benchmark with five task suites: LIBERO-Goal, LIBERO-Spatial, LIBERO-Object, LIBERO-Long (10 tasks each with 50 demonstrations), and LIBERO-90 (90 tasks for large-scale evaluation). Performance is measured by average Success Rate (SR) across 50 held-out test scenarios per task. RoboTwin1.0 provides 17 bimanual tasks, while RoboTwin2.0 extends to 50 tasks with 731 object instances and comprehensive domain randomization (clutter, lighting, background, tabletop height, language instructions), enhancing task diversity and sim-to-real transfer. For RoboTwin2.0, we use the Agilex Piper robotic arm and domain-randomized task settings, with each task evaluated on 100 held-out test scenarios. We select 12 tasks in RoboTwin2.0 and categorize them into 4 horizon levels based on average step counts, as detailed in Table 7.

Backbones We apply **SimpleVLA-RL** to OpenVLA-OFT (Kim et al., 2025), a state-of-theart auto-regressive VLA model with high performance and inference efficiency. Built on Open-VLA (Kim et al., 2024), it uses vision encoders and LLaMA2-7B (Touvron et al., 2023) as the backbone with action chunk and parallel decoding, making it suitable for online RL's frequent inference requirements. Our implementation of the OpenVLA-OFT differs from the official version (see Appendix F.2 for modifications and Appendix F.3 for hyperparameters).

Baselines We compare with advanced VLA models: UniVLA (Bu et al., 2025b), RDT-1B (Liu et al., 2024), π_0 (Black et al., 2024), π_{fast} (Pertsch et al., 2025), Nora (Hung et al., 2025), Open-VLA (Kim et al., 2024), Octo (Team et al., 2024), DP (Chi et al., 2024) and DP3 (Ze et al., 2024).

3.2 Main Results

We evaluate **SimpleVLA-RL** on LIBERO, RoboTwin1.0, and RoboTwin2.0 using a two-stage paradigm: SFT followed by **SimpleVLA-RL** on OpenVLA-OFT, while baselines use SFT only. For LIBERO's four task suites, we perform SFT with 500 demonstrations per task suite, then RL on 500 simulation scenarios. For RoboTwin1.0, we use 50 demonstrations per task for single-task SFT, then 100 scenarios per task for RL. For RoboTwin2.0, we use 1,000 demonstrations per task for single-task SFT, then 1,000 scenarios per task for RL.

Table 2: Main results of different VLA models on RoboTwin2.0, organized by task horizon.

Short Horizon Tasks (100-130 Steps)						
Model	Lift Pot	Beat Hammer Block	Pick Dual Bottles	Place Phone Stand	Avg	
π_0 RDT	51.0	59.0	50.0	22.0	45.5	
	45.0	22.0	18.0	13.0	24.5	
OpenVLA-OFT	10.1	28.1	29.7	17.1	21.3	
w/ ours	64.1	87.5	68.3	39.6	64.9	
Δ	+54.0	+59.4	+38.6	+22.5	+43.6	

Medium Horizon Tasks (150-230 Steps)						
Model	Move Can Pot	Place A2B Left	Place Empty Cup	Handover Mic	Avg	
π_0	41.0	38.0	84.0	96.0	64.8	
RDT	33.0	21.0	42.0	95.0	47.8	
OpenVLA-OFT	28.1	37.5	77.3	45.3	47.1	
w/ ours	61.2	45.3	94.2	89.2	72.5	
Δ	+33.1	+7.8	+16.9	+43.9	+25.4	

Long (280, 320 Stone)	& Extra Long Horizon	Tocks (450, 650 Stops)
LUII2 (200-320 SIEDS)	& EXITA LONG HOUZON	1 asks (450-050 5160s)

Model	Handover Block	k Stack Bowls	Two Blocks Rank Rgb	Put Bottles Dustbin	Avg
π_0 RDT	39.0 26.0	53.0 42.0	45.0 17.0	54.0 26.0	47.8 27.8
OpenVLA-OFT		40.6	70.2	42.2	46.5
w/ ours	57.8	75.8	81.3	60.9	69.0
Δ	+24.7	+35.2	+11.1	+18.7	+22.4
Overall Avg		RDT: 33.3	$\mathbf{r_0}$: 52.7 OpenVLA-OF	r: 38.3 w/ ours : 68.8	+30.5

Tables 1, 2, and 3 present results on LIBERO, RoboTwin1.0, and RoboTwin2.0 benchmarks. On LIBERO, SimpleVLA-RL improves OpenVLA-OFT from 91% to 99% average success rate, achieving SoTA performance and surpassing models like π_0 and UniVLA. For long-horizon tasks in LIBERO-Long, SimpleVLA-RL reaches 98.5% success rate, with a 12% improvement over baseline and 13.3% over π_0 . On RoboTwin1.0's dual-arm tasks, SimpleVLA-RL achieves 30.6% gains

Table 3: Main results on LIBERO.

Model	LIBERO					
1120401	Spatial	Object	Goal	Long	Avg	
Octo	78.9	85.7	84.6	51.1	75.1	
OpenVLA	84.7	88.4	79.2	53.7	76.5	
Nora	92.2	95.4	89.4	74.6	87.9	
π_0 + FAST	96.4	96.8	88.6	60.2	85.5	
π_0	96.8	98.8	95.8	85.2	94.2	
UniVLA	96.5	96.8	95.6	92.0	95.2	
OpenVLA-OFT	91.6	95.3	90.6	86.5	91.0	
w/ ours	99.4	99.1	99.2	98.5	99.1	
Δ	+7.8	+3.8	+8.6	+12.0	+8.1	

(39.8% to 70.4%). Across RoboTwin2.0's 12 tasks, SimpleVLA-RL delivers 80% relative improvement (38.3% to 68.8%), outperforming SoTA methods including π_0 (52.7%) and RDT (33.3%). Even on Extra-Long-Horizon tasks like "Blocks Rank Rgb" and "Put Bottles Dustbin", SimpleVLA-RL achieves 11.1% and 18.7% point gains respectively, demonstrating effectiveness across all horizon levels. These results validate that SimpleVLA-RL consistently improves model performance across diverse benchmarks without requiring additional demonstration data, proving the effectiveness of outcome-level rewards even for complex long-horizon tasks.

4 ANALYSIS

In this section, we analyze the role of **SimpleVLA-RL** in addressing three key challenges that hinder the further advancement and scaling of the VLA model: **data**, **generalization**, **and real-world tasks**. Below are several key takeaways:

Takeaways

- 1. **Data: SimpleVLA-RL** can significantly reduce reliance on demonstration data, effectively alleviating the data scarcity bottleneck that constrains VLA scaling (§ **4.1**).
- 2. **Generalization:** Compared to SFT, **SimpleVLA-RL** demonstrates strong generalization in spatial configurations, object types, and task settings (§ **4.2**).
- 3. **Real-world Task: SimpleVLA-RL** exhibits strong sim-to-real transfer, with large-scale simulation training remarkably improving real-world performance, indicating a promising path for scaling up real-world policy (§ **4.3**).

4.1 Overcoming Data Scarcity

Developing foundation VLA models for manipulation tasks requires large-scale demonstration data for training (Liu et al., 2024; Black et al., 2024; Intelligence et al., 2025). This data scaling paradigm has been proven in the NLP area (Hoffmann et al., 2022; Achiam et al., 2023; Touvron et al., 2023). However, acquiring high-quality trajectory data for embodied manipulation tasks remains expensive and difficult, creating a fundamental bottleneck for VLA model development (Bi et al., 2025; Zhong et al., 2025). Therefore, we investigate whether **SimpleVLA-RL** can enhance VLA models even with extremely limited demonstration trajectories to overcome this limitation.

Settings To simulate scenarios with scarce demonstration data, we finetune OpenVLA-OFT using only one demonstration data per task, denoted as *One-Trajectory SFT*. Given that each of the four LIBERO task suites contains 10 distinct tasks, we utilize merely 10 demonstration data per task suite. For comparison, we also conduct an experiment using all available demonstration data for each task, 500 per task suite, denoted as *Full-Trajectory SFT*. Following both *One-Trajectory SFT* and *Full-Trajectory SFT*, we apply **SimpleVLA-RL** on the SFT model.

Results As shown in Table 4, SFT performance degrades significantly with limited data. Under *One-Trajectory SFT*, success rates drop below 63.6% for LIBERO-Spatial/Object/Goal and to only 17.3% for LIBERO-Long, compared to 91.0% average under *Full-Trajectory SFT*. Remarkably, applying SimpleVLA-RL to *One-Trajectory SFT* models increases the average success rate from 48.9% to 96.9%, surpassing even *Full-Trajectory SFT*'s 91.0%. LIBERO-Long improves dramatically from 17.3% to 91.7%, while the other three task suites all

Table 4: Comparisons between One-Trajectory and Full-Trajectory SFT on LIBERO.

Model	LIBERO						
1,10401	Spatial	Object	Goal	Long	Avg		
	One-	-Trajectory	SFT				
OpenVLA-OFT	63.6	54.9	59.6	17.3	48.9		
w/ ours	98.2	98.7	98.8	91.7	96.9		
Δ	+34.6	+43.8	+39.2	+74.4	+48.0		
	Full-	Trajectory	SFT				
OpenVLA-OFT	91.6	95.3	90.6	86.5	91.0		
w/ ours	99.4	99.1	99.2	98.5	99.1		
Δ	+7.8	+3.8	+8.6	+12.0	+8.1		

exceed 98%. The performance gap between *One-Trajectory SFT* + RL (96.9%) and Full-Trajectory SFT + RL (99.1%) is merely 2.2%. The results demonstrate that **SimpleVLA-RL** can substantially improve performance even in data-scarce scenarios, suggesting that online RL enables further scaling of VLA training through trial-and-error exploration, even with minimal demonstration data.

4.2 GENERALIZATION ANALYSIS

The generalization ability of VLA models remains a key challenge (Intelligence et al., 2025; Zhong et al., 2025; Liu et al., 2025a). This subsection evaluates how SFT and online RL methods like **SimpleVLA-RL** affect VLA generalization across three dimensions: spatial (LIBERO-Spatial), objects (LIBERO-Object), and tasks (LIBERO-Goal).

Settings We experiment on three LIBERO task suites (Spatial, Object, Goal), each containing ten tasks. For each suite, we randomly select nine tasks as seen tasks for RL or SFT training, while reserving the remaining task as the unseen task for out-of-distribution evaluation. For both methods, we first fine-tune OpenVLA-OFT under the *One-Trajectory SFT* setting to obtain a base model with non-zero success rates, since the original model achieves 0% on LIBERO and is incapable of performing online RL. For SFT, we further fine-tune the *One-Trajectory SFT* base model (§4.1) using 450 demonstrations from 9 seen tasks on each task suite. For RL, we perform **SimpleVLA-RL** on the *One-Trajectory SFT* base model using 450 scenarios from 9 seen tasks. We plot how unseen task performance evolves as training task success rates increase during training.

Results Figure 4 presents the results. While both SFT and RL achieve over 90% success rates on training tasks, their performance on unseen tasks diverges significantly. As training progresses, SimpleVLA-RL shows consistent improvement on unseen tasks across all settings, whereas SFT suffers from severe overfitting, often experiencing catastrophic forgetting with success rates of unseen tasks dropping to 0%. **On LIBERO-Goal**, SFT immediately drops to 0% on all three unseen tasks at training onset, likely because these tasks involve diverse objects and manipulation strategies with minimal transferable components. In contrast, SimpleVLA-RL maintains performance and achieves 5%-15% improvements. **On LIBERO-Object**, SFT improves only on Unseen Task 3 (57.8% to 74.6%) while failing on the other two. SimpleVLA-RL improves across all three tasks,

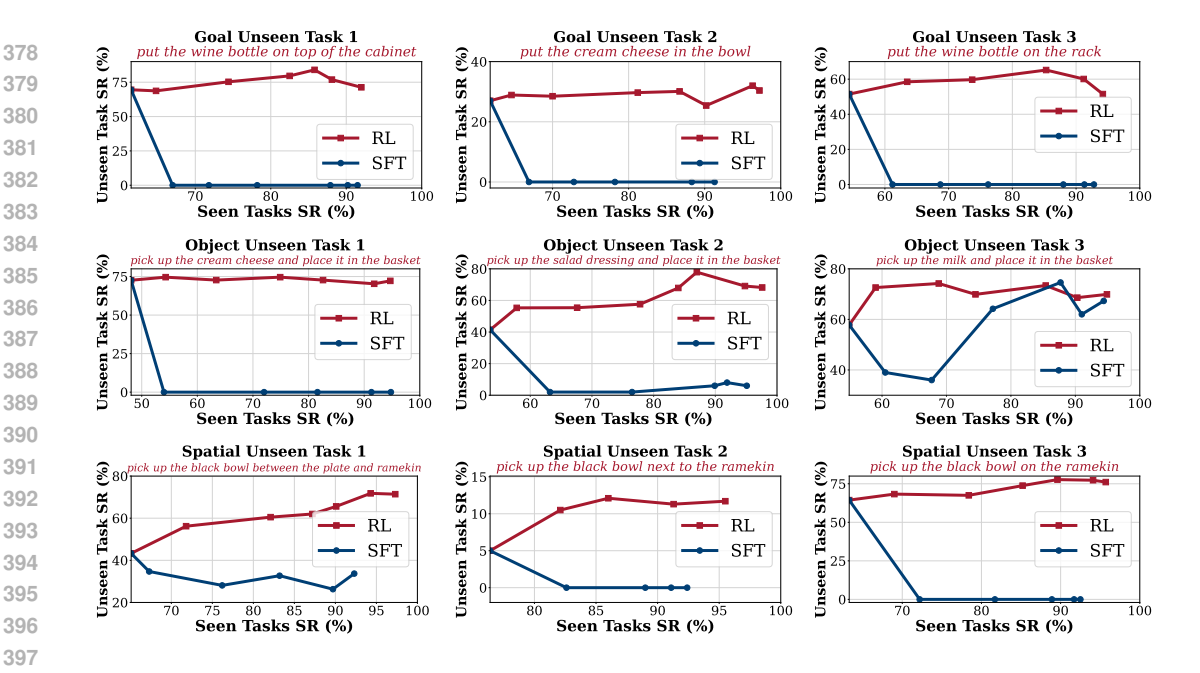


Figure 4: Generalization Analysis on LIBERO: Goal Unseen (**Top**), Object Unseen (**Middle**), Spatial Unseen (**Bottom**).

with notable gains of 36.5% on Task 2 and 16.4% on Task 3. **On LIBERO-Spatial**, SFT degrades by 10% on Unseen Task 1 and completely fails on the remaining tasks, while SimpleVLA-RL improves Task 1 performance from 43.3% to 71.8% and achieves 7.1% and 13.3% gains on the other tasks. These results demonstrate that RL training enables VLA models to retain previously acquired capabilities while learning generalizable skills from diverse tasks.

4.3 REAL-WORLD EXPERIMENTS

Table 5: Real-world experiment (sim2real) results.

	Stack Bowls	Place Empty Cup	Pick Bottle	Click Bell	Avg
RDT	60.0	4.0	10.0	20.0	23.5
OpenVLA-OFT		2.0	0.0	30.0	17.5
w/ ours	70.0	10.0	14.0	60.0	38.5
Δ	+32.0	+8.0	+14.0	+30.0	+21.0

To evaluate the real-world effectiveness of **SimpleVLA-RL**, we conduct sim-to-real experiments on four RoboTwin2.0 tasks (detailed in Appendix F.1): Stack Bowls, Handover Block, Pick Bottle, and Click Bell. We employ OpenVLA-OFT as the policy model, RDT as the baseline model, and execute on two AgileX Piper robotic arms. For each task, we first use 1000 simulation trajectories for SFT. Then we apply **SimpleVLA-RL** on the SFT model using 1000 simulation scenarios to obtain an RL model. The entire training process uses only simulation data without any real-world demonstrations. We evaluate both the SFT and RL models on clean tabletops with unseen backgrounds in the real world. Each task is tested with 50 trials. The RDT baseline model only undergoes the SFT stage.

The sim2real results in Table 5 demonstrate that **SimpleVLA-RL** significantly improves the real-world success rates of VLA models, with an average improvement from 17.5% to 38.5%, surpassing RDT's 23.5%. For instance, in the Stack Bowls task, **SimpleVLA-RL** achieves a 84% relative improvement, lifting performance from 38% to 70%. On the Pick Bottle task, which demands higher action precision, as the bottle will fall if the robotic arm is not perfectly aligned on the first attempt, the SFT model fails completely while **SimpleVLA-RL** achieves a 14% success rate. This demonstrates RL's effectiveness in improving action precision. Using **SimpleVLA-RL** for low-cost, large-scale, and highly parallel RL training in simulation, we significantly improve the real-world performance of simulation-trained VLA models. This demonstrates a promising path for scaling

real-world policies: using rich simulation assets and high-fidelity simulators for cost-effective RL training to achieve superior performance in real-world deployment.

5 DISCUSSIONS

5.1 "PUSHCUT": EMERGENCE OF NEW PATTERNS THROUGH RL

Task: Move Can Pot SFT Grasp RL

SFT Grasp

RL

Push

Task: Place A2B Right

(a) "move can pot" task: Model learned to push the can to the pot (bottom) instead of grasp-move-place in the demonstration data (top).

(b) "place a2b right" task: Model learned to push A to B's right (bottom) instead of demonstrated grasp-move-place (top).

Figure 5: Illustration of "pushcut". Emergent pushing behaviors through RL in RoboTwin2.0 tasks.

During RL training with **SimpleVLA-RL**, we observe an emergent behavior we call "pushcut" (a push-driven shortcut), where the VLA model discovers novel strategies absent from the demonstration data. In the *move can pot* task of RoboTwin2.0, all demonstrations follow a grasp—move—place strategy (Figure 5a, top). However, after RL training, the model autonomously discovers a more efficient solution: directly pushing the can to the target location instead of grasping it (Figure 5a, bottom). Similar behaviors emerge in the *place a2b left/right* task, where the RL-trained model learns to push Object A into position rather than following the demonstrated grasp-move-place approach (Figure 5b).

This "pushcut" phenomenon parallels the "Aha Moment" in DeepSeek-R1 (Guo et al., 2025a), as both emerge through RL-driven exploration. This phenomenon highlights the fundamental distinction between SFT and RL. While SFT merely replicates patterns from demonstrations, RL enables the discovery of novel strategies through reward-driven exploration. The outcome-level reward design is crucial here: since both grasping and pushing receive equal rewards upon task completion, the sparse reward structure avoids procedural constraints, allowing the agent to explore freely and discover unexpected yet effective solutions.

5.2 FAILURE MODES OF SIMPLEVLA-RL

We conduct ablation studies to identify failure conditions and key influencing factors of **SimpleVLA-RL** (see Appendix C for full results and analysis). Our experiments reveal that model priors are the critical factor determining RL effectiveness. RL fails completely when the base model lacks initial task capability (0% success rate). Furthermore, we find a performance threshold: when initial success rates are too low (< 5%), RL improvements remain negligible, while stronger initial models achieve substantially better final performance after RL training.

6 CONCLUSION

In this work, we present **SimpleVLA-RL**, an RL framework tailored for VLA models that extends veRL with VLA-specific trajectory sampling and parallelized training—inference—rendering capabilities. **SimpleVLA-RL** demonstrates significant improvements in data efficiency, generalization, and sim-to-real transfer. These results across LIBERO and RoboTwin benchmarks highlight RL's potential to both alleviate data scarcity and substantially enhance VLA generalization, paving the way for more autonomous and adaptable robotic models.

ETHICS STATEMENT

This work presents **SimpleVLA-RL**, a reinforcement learning framework for improving Vision-Language-Action models in robotic manipulation. Our research aims to advance autonomous robotics for beneficial applications in manufacturing, healthcare, and assistive technologies. We conduct experiments exclusively in simulation environments and controlled laboratory settings with standard manipulation tasks, ensuring safe development practices. Our approach reduces reliance on large-scale human-operated data collection, minimizing both human labor costs and potential safety risks associated with extensive teleoperation. By enabling more sample-efficient training and better generalization, **SimpleVLA-RL** promotes environmentally conscious research through reduced computational requirements compared to scaling supervised learning alone. All experiments use publicly available benchmarks and models to ensure transparent, reproducible research.

REPRODUCIBILITY STATEMENT

We provide comprehensive details to ensure reproducibility of our work. The complete algorithmic formulation of **SimpleVLA-RL** and training procedures are described in Section 2, including trajectory sampling, loss computation, and exploration strategies. All experimental configurations, model hyperparameters, hardware specifications, and robotic arm setups are detailed in Appendix F. We provide implementation specifics built upon the open-source veRL framework, evaluation protocols for LIBERO and RoboTwin benchmarks, and baseline comparisons. Additionally, we include ablation study configurations and real-world deployment settings. All mathematical formulations, implementation details, and experimental configurations necessary for reproducing our results are included in the paper.

REFERENCES

- Josh Achiam, Steven Adler, Sandhini Agarwal, Lama Ahmad, Ilge Akkaya, Florencia Leoni Aleman, Diogo Almeida, Janko Altenschmidt, Sam Altman, Shyamal Anadkat, et al. Gpt-4 technical report. arXiv preprint arXiv:2303.08774, 2023.
- Arash Ahmadian, Chris Cremer, Matthias Gallé, Marzieh Fadaee, Julia Kreutzer, Olivier Pietquin, Ahmet Üstün, and Sara Hooker. Back to basics: Revisiting reinforce style optimization for learning from human feedback in llms. *arXiv preprint arXiv:2402.14740*, 2024.
- Chenxin An, Zhihui Xie, Xiaonan Li, Lei Li, Jun Zhang, Shansan Gong, Ming Zhong, Jingjing Xu, Xipeng Qiu, Mingxuan Wang, and Lingpeng Kong. Polaris: A post-training recipe for scaling reinforcement learning on advanced reasoning models, 2025. URL https://hkunlp.github.io/blog/2025/Polaris.
- Hongzhe Bi, Lingxuan Wu, Tianwei Lin, Hengkai Tan, Zhizhong Su, Hang Su, and Jun Zhu. H-rdt: Human manipulation enhanced bimanual robotic manipulation. *arXiv preprint arXiv:2507.23523*, 2025.
- Kevin Black, Noah Brown, Danny Driess, Adnan Esmail, Michael Equi, Chelsea Finn, Niccolo Fusai, Lachy Groom, Karol Hausman, Brian Ichter, et al. pi_0: A vision-language-action flow model for general robot control. *arXiv preprint arXiv:2410.24164*, 2024.
- Serena Booth, W Bradley Knox, Julie Shah, Scott Niekum, Peter Stone, and Alessandro Allievi. The perils of trial-and-error reward design: misdesign through overfitting and invalid task specifications. In *Proceedings of the AAAI Conference on Artificial Intelligence*, volume 37, pp. 5920–5929, 2023.
- Qingwen Bu, Jisong Cai, Li Chen, Xiuqi Cui, Yan Ding, Siyuan Feng, Shenyuan Gao, Xindong He, Xu Huang, Shu Jiang, et al. Agibot world colosseo: A large-scale manipulation platform for scalable and intelligent embodied systems. *arXiv preprint arXiv:2503.06669*, 2025a.
- Qingwen Bu, Yanting Yang, Jisong Cai, Shenyuan Gao, Guanghui Ren, Maoqing Yao, Ping Luo, and Hongyang Li. Univla: Learning to act anywhere with task-centric latent actions. *arXiv* preprint *arXiv*:2505.06111, 2025b.

- Chilam Cheang, Sijin Chen, Zhongren Cui, Yingdong Hu, Liqun Huang, Tao Kong, Hang Li, Yifeng
 Li, Yuxiao Liu, Xiao Ma, et al. Gr-3 technical report. arXiv preprint arXiv:2507.15493, 2025.
 - Tianxing Chen, Zanxin Chen, Baijun Chen, Zijian Cai, Yibin Liu, Qiwei Liang, Zixuan Li, Xianliang Lin, Yiheng Ge, Zhenyu Gu, et al. Robotwin 2.0: A scalable data generator and benchmark with strong domain randomization for robust bimanual robotic manipulation. *arXiv* preprint arXiv:2506.18088, 2025a.
 - William Chen, Suneel Belkhale, Suvir Mirchandani, Oier Mees, Danny Driess, Karl Pertsch, and Sergey Levine. Training strategies for efficient embodied reasoning. *arXiv preprint arXiv:2505.08243*, 2025b.
 - Yuhui Chen, Shuai Tian, Shugao Liu, Yingting Zhou, Haoran Li, and Dongbin Zhao. Conft: A reinforced fine-tuning method for vla models via consistency policy. *arXiv preprint arXiv:2502.05450*, 2025c.
 - Zengjue Chen, Runliang Niu, He Kong, and Qi Wang. Tgrpo: Fine-tuning vision-language-action model via trajectory-wise group relative policy optimization. *arXiv preprint arXiv:2506.08440*, 2025d.
 - Cheng Chi, Zhenjia Xu, Siyuan Feng, Eric Cousineau, Yilun Du, Benjamin Burchfiel, Russ Tedrake, and Shuran Song. Diffusion policy: Visuomotor policy learning via action diffusion. *The International Journal of Robotics Research*, 2024.
 - Ganqu Cui, Lifan Yuan, Zefan Wang, Hanbin Wang, Wendi Li, Bingxiang He, Yuchen Fan, Tianyu Yu, Qixin Xu, Weize Chen, et al. Process reinforcement through implicit rewards. *arXiv preprint arXiv:2502.01456*, 2025a.
 - Ganqu Cui, Yuchen Zhang, Jiacheng Chen, Lifan Yuan, Zhi Wang, Yuxin Zuo, Haozhan Li, Yuchen Fan, Huayu Chen, Weize Chen, et al. The entropy mechanism of reinforcement learning for reasoning language models. *arXiv preprint arXiv:2505.22617*, 2025b.
 - Gustavo H De Rosa and Joao P Papa. A survey on text generation using generative adversarial networks. *Pattern Recognition*, 119:108098, 2021.
 - Roya Firoozi, Johnathan Tucker, Stephen Tian, Anirudha Majumdar, Jiankai Sun, Weiyu Liu, Yuke Zhu, Shuran Song, Ashish Kapoor, Karol Hausman, et al. Foundation models in robotics: Applications, challenges, and the future. *The International Journal of Robotics Research*, 44(5): 701–739, 2025.
 - Jensen Gao, Annie Xie, Ted Xiao, Chelsea Finn, and Dorsa Sadigh. Efficient data collection for robotic manipulation via compositional generalization. *arXiv preprint arXiv:2403.05110*, 2024.
 - Haoran Geng, Feishi Wang, Songlin Wei, Yuyang Li, Bangjun Wang, Boshi An, Charlie Tianyue Cheng, Haozhe Lou, Peihao Li, Yen-Jen Wang, et al. Roboverse: Towards a unified platform, dataset and benchmark for scalable and generalizable robot learning. *arXiv preprint arXiv:2504.18904*, 2025.
 - Daya Guo, Dejian Yang, Haowei Zhang, Junxiao Song, Ruoyu Zhang, Runxin Xu, Qihao Zhu, Shirong Ma, Peiyi Wang, Xiao Bi, et al. Deepseek-r1: Incentivizing reasoning capability in llms via reinforcement learning. *arXiv* preprint arXiv:2501.12948, 2025a.
 - Yanjiang Guo, Jianke Zhang, Xiaoyu Chen, Xiang Ji, Yen-Jen Wang, Yucheng Hu, and Jianyu Chen. Improving vision-language-action model with online reinforcement learning. *arXiv preprint arXiv:2501.16664*, 2025b.
 - Abhishek Gupta, Vikash Kumar, Corey Lynch, Sergey Levine, and Karol Hausman. Relay policy learning: Solving long-horizon tasks via imitation and reinforcement learning. *arXiv* preprint *arXiv*:1910.11956, 2019.
 - Dylan Hadfield-Menell, Smitha Milli, Pieter Abbeel, Stuart J Russell, and Anca Dragan. Inverse reward design. *Advances in neural information processing systems*, 30, 2017.

- Jordan Hoffmann, Sebastian Borgeaud, Arthur Mensch, Elena Buchatskaya, Trevor Cai, Eliza Rutherford, Diego de Las Casas, Lisa Anne Hendricks, Johannes Welbl, Aidan Clark, et al. Training compute-optimal large language models. *arXiv preprint arXiv:2203.15556*, 2022.
 - Yucheng Hu, Yanjiang Guo, Pengchao Wang, Xiaoyu Chen, Yen-Jen Wang, Jianke Zhang, Koushil Sreenath, Chaochao Lu, and Jianyu Chen. Video prediction policy: A generalist robot policy with predictive visual representations. *arXiv* preprint arXiv:2412.14803, 2024.
 - Chia-Yu Hung, Qi Sun, Pengfei Hong, Amir Zadeh, Chuan Li, U Tan, Navonil Majumder, Soujanya Poria, et al. Nora: A small open-sourced generalist vision language action model for embodied tasks. *arXiv preprint arXiv:2504.19854*, 2025.
 - Julian Ibarz, Jie Tan, Chelsea Finn, Mrinal Kalakrishnan, Peter Pastor, and Sergey Levine. How to train your robot with deep reinforcement learning: lessons we have learned. *The International Journal of Robotics Research*, 40(4-5):698–721, 2021.
 - Physical Intelligence, Kevin Black, Noah Brown, James Darpinian, Karan Dhabalia, Danny Driess, Adnan Esmail, Michael Equi, Chelsea Finn, Niccolo Fusai, et al. pi_ {0.5}: a vision-language-action model with open-world generalization. arXiv preprint arXiv:2504.16054, 2025.
 - Aaron Jaech, Adam Kalai, Adam Lerer, Adam Richardson, Ahmed El-Kishky, Aiden Low, Alec Helyar, Aleksander Madry, Alex Beutel, Alex Carney, et al. Openai o1 system card. *arXiv* preprint arXiv:2412.16720, 2024.
 - Zhenyu Jiang, Yuqi Xie, Kevin Lin, Zhenjia Xu, Weikang Wan, Ajay Mandlekar, Linxi Fan, and Yuke Zhu. Dexmimicgen: Automated data generation for bimanual dexterous manipulation via imitation learning. *arXiv preprint arXiv:2410.24185*, 2024.
 - Moo Jin Kim, Karl Pertsch, Siddharth Karamcheti, Ted Xiao, Ashwin Balakrishna, Suraj Nair, Rafael Rafailov, Ethan Foster, Grace Lam, Pannag Sanketi, et al. Openvla: An open-source vision-language-action model. *arXiv preprint arXiv:2406.09246*, 2024.
 - Moo Jin Kim, Chelsea Finn, and Percy Liang. Fine-tuning vision-language-action models: Optimizing speed and success. *arXiv preprint arXiv:2502.19645*, 2025.
 - W Bradley Knox, Alessandro Allievi, Holger Banzhaf, Felix Schmitt, and Peter Stone. Reward (mis) design for autonomous driving. *Artificial Intelligence*, 316:103829, 2023.
 - Oliver Kroemer, Scott Niekum, and George Konidaris. A review of robot learning for manipulation: Challenges, representations, and algorithms. *Journal of machine learning research*, 22(30):1–82, 2021.
 - Mengqi Liao, Xiangyu Xi, Ruinian Chen, Jia Leng, Yangen Hu, Ke Zeng, Shuai Liu, and Huaiyu Wan. Enhancing efficiency and exploration in reinforcement learning for llms. *arXiv preprint arXiv:2505.18573*, 2025.
 - Bo Liu, Yifeng Zhu, Chongkai Gao, Yihao Feng, Qiang Liu, Yuke Zhu, and Peter Stone. Libero: Benchmarking knowledge transfer for lifelong robot learning. *Advances in Neural Information Processing Systems*, 36:44776–44791, 2023.
 - Jijia Liu, Feng Gao, Bingwen Wei, Xinlei Chen, Qingmin Liao, Yi Wu, Chao Yu, and Yu Wang. What can rl bring to vla generalization? an empirical study. *arXiv preprint arXiv:2505.19789*, 2025a.
 - Mingjie Liu, Shizhe Diao, Ximing Lu, Jian Hu, Xin Dong, Yejin Choi, Jan Kautz, and Yi Dong. Prorl: Prolonged reinforcement learning expands reasoning boundaries in large language models. *arXiv preprint arXiv:2505.24864*, 2025b.
 - Songming Liu, Lingxuan Wu, Bangguo Li, Hengkai Tan, Huayu Chen, Zhengyi Wang, Ke Xu, Hang Su, and Jun Zhu. Rdt-1b: a diffusion foundation model for bimanual manipulation. *arXiv* preprint *arXiv*:2410.07864, 2024.

- Zichen Liu, Changyu Chen, Wenjun Li, Penghui Qi, Tianyu Pang, Chao Du, Wee Sun Lee, and Min Lin. Understanding r1-zero-like training: A critical perspective. *arXiv preprint arXiv:2503.20783*, 2025c.
 - Zihan Liu, Zhuolin Yang, Yang Chen, Chankyu Lee, Mohammad Shoeybi, Bryan Catanzaro, and Wei Ping. Acereason-nemotron 1.1: Advancing math and code reasoning through sft and rl synergy. *arXiv preprint arXiv:2506.13284*, 2025d.
 - Guanxing Lu, Wenkai Guo, Chubin Zhang, Yuheng Zhou, Haonan Jiang, Zifeng Gao, Yansong Tang, and Ziwei Wang. Vla-rl: Towards masterful and general robotic manipulation with scalable reinforcement learning. *arXiv* preprint arXiv:2505.18719, 2025.
 - Jianlan Luo, Zheyuan Hu, Charles Xu, You Liang Tan, Jacob Berg, Archit Sharma, Stefan Schaal, Chelsea Finn, Abhishek Gupta, and Sergey Levine. Serl: A software suite for sample-efficient robotic reinforcement learning. arXiv preprint arXiv:2401.16013, 2025.
 - Yecheng Jason Ma, Shagun Sodhani, Dinesh Jayaraman, Osbert Bastani, Vikash Kumar, and Amy Zhang. Vip: Towards universal visual reward and representation via value-implicit pre-training. arXiv preprint arXiv:2210.00030, 2022.
 - Yecheng Jason Ma, William Liang, Guanzhi Wang, De-An Huang, Osbert Bastani, Dinesh Jayaraman, Yuke Zhu, Linxi Fan, and Anima Anandkumar. Eureka: Human-level reward design via coding large language models. *arXiv preprint arXiv:2310.12931*, 2023.
 - Yao Mu, Tianxing Chen, Shijia Peng, Zanxin Chen, Zeyu Gao, Yude Zou, Lunkai Lin, Zhiqiang Xie, and Ping Luo. Robotwin: Dual-arm robot benchmark with generative digital twins (early version). In *European Conference on Computer Vision*, pp. 264–273. Springer, 2025.
 - Long Ouyang, Jeffrey Wu, Xu Jiang, Diogo Almeida, Carroll Wainwright, Pamela Mishkin, Chong Zhang, Sandhini Agarwal, Katarina Slama, Alex Ray, et al. Training language models to follow instructions with human feedback. *Advances in neural information processing systems*, 35: 27730–27744, 2022.
 - Abby O'Neill, Abdul Rehman, Abhiram Maddukuri, Abhishek Gupta, Abhishek Padalkar, Abraham Lee, Acorn Pooley, Agrim Gupta, Ajay Mandlekar, Ajinkya Jain, et al. Open x-embodiment: Robotic learning datasets and rt-x models: Open x-embodiment collaboration 0. In 2024 IEEE International Conference on Robotics and Automation (ICRA), pp. 6892–6903. IEEE, 2024.
 - Karl Pertsch, Kyle Stachowicz, Brian Ichter, Danny Driess, Suraj Nair, Quan Vuong, Oier Mees, Chelsea Finn, and Sergey Levine. Fast: Efficient action tokenization for vision-language-action models. *arXiv preprint arXiv:2501.09747*, 2025.
 - Rafael Rafailov, Archit Sharma, Eric Mitchell, Christopher D Manning, Stefano Ermon, and Chelsea Finn. Direct preference optimization: Your language model is secretly a reward model. Advances in Neural Information Processing Systems, 36:53728–53741, 2023.
 - Matthew Renze. The effect of sampling temperature on problem solving in large language models. In *Findings of the association for computational linguistics: EMNLP 2024*, pp. 7346–7356, 2024.
 - Stephane Ross and Drew Bagnell. Efficient reductions for imitation learning. In Yee Whye Teh and Mike Titterington (eds.), *Proceedings of the Thirteenth International Conference on Artificial Intelligence and Statistics*, volume 9 of *Proceedings of Machine Learning Research*, pp. 661–668, Chia Laguna Resort, Sardinia, Italy, 13–15 May 2010. PMLR. URL https://proceedings.mlr.press/v9/ross10a.html.
 - Ranjan Sapkota, Yang Cao, Konstantinos I Roumeliotis, and Manoj Karkee. Vision-language-action models: Concepts, progress, applications and challenges. *arXiv preprint arXiv:2505.04769*, 2025.
 - John Schulman, Sergey Levine, Pieter Abbeel, Michael Jordan, and Philipp Moritz. Trust region policy optimization. In *International conference on machine learning*, pp. 1889–1897. PMLR, 2015.
 - John Schulman, Filip Wolski, Prafulla Dhariwal, Alec Radford, and Oleg Klimov. Proximal policy optimization algorithms. *arXiv preprint arXiv:1707.06347*, 2017a.

- John Schulman, Filip Wolski, Prafulla Dhariwal, Alec Radford, and Oleg Klimov. Proximal policy optimization algorithms. 2017b. URL https://arxiv.org/abs/1707.06347.
 - Zhihong Shao, Peiyi Wang, Qihao Zhu, Runxin Xu, Junxiao Song, Xiao Bi, Haowei Zhang, Mingchuan Zhang, YK Li, Y Wu, et al. Deepseekmath: Pushing the limits of mathematical reasoning in open language models. *arXiv preprint arXiv:2402.03300*, 2024.
 - Guangming Sheng, Chi Zhang, Zilingfeng Ye, Xibin Wu, Wang Zhang, Ru Zhang, Yanghua Peng, Haibin Lin, and Chuan Wu. Hybridflow: A flexible and efficient rlhf framework. *arXiv preprint arXiv:* 2409.19256, 2024.
 - Taiwei Shi, Yiyang Wu, Linxin Song, Tianyi Zhou, and Jieyu Zhao. Efficient reinforcement finetuning via adaptive curriculum learning. *arXiv preprint arXiv:2504.05520*, 2025.
 - Junyang Shu, Zhiwei Lin, and Yongtao Wang. Rftf: Reinforcement fine-tuning for embodied agents with temporal feedback. *arXiv preprint arXiv:2505.19767*, 2025.
 - Shuhan Tan, Kairan Dou, Yue Zhao, and Philipp Krähenbühl. Interactive post-training for vision-language-action models. *arXiv preprint arXiv:2505.17016*, 2025.
 - Gemini Robotics Team, Saminda Abeyruwan, Joshua Ainslie, Jean-Baptiste Alayrac, Montserrat Gonzalez Arenas, Travis Armstrong, Ashwin Balakrishna, Robert Baruch, Maria Bauza, Michiel Blokzijl, et al. Gemini robotics: Bringing ai into the physical world. *arXiv preprint arXiv:2503.20020*, 2025a.
 - Kimi Team, Angang Du, Bofei Gao, Bowei Xing, Changjiu Jiang, Cheng Chen, Cheng Li, Chenjun Xiao, Chenzhuang Du, Chonghua Liao, et al. Kimi k1. 5: Scaling reinforcement learning with llms. *arXiv preprint arXiv:2501.12599*, 2025b.
 - Octo Model Team, Dibya Ghosh, Homer Walke, Karl Pertsch, Kevin Black, Oier Mees, Sudeep Dasari, Joey Hejna, Tobias Kreiman, Charles Xu, et al. Octo: An open-source generalist robot policy. *arXiv preprint arXiv:2405.12213*, 2024.
 - RLinf Team. Rlinf: Reinforcement learning infrastructure for agentic ai. https://github.com/RLinf/RLinf, 2025. GitHub repository.
 - Hugo Touvron, Louis Martin, Kevin Stone, Peter Albert, Amjad Almahairi, Yasmine Babaei, Nikolay Bashlykov, Soumya Batra, Prajjwal Bhargava, Shruti Bhosale, et al. Llama 2: Open foundation and fine-tuned chat models. *arXiv preprint arXiv:2307.09288*, 2023.
 - Luong Trung, Xinbo Zhang, Zhanming Jie, Peng Sun, Xiaoran Jin, and Hang Li. Reft: Reasoning with reinforced fine-tuning. In *Proceedings of the 62nd Annual Meeting of the Association for Computational Linguistics (Volume 1: Long Papers)*, pp. 7601–7614, 2024.
 - Yihao Wang, Pengxiang Ding, Lingxiao Li, Can Cui, Zirui Ge, Xinyang Tong, Wenxuan Song, Han Zhao, Wei Zhao, Pengxu Hou, Siteng Huang, Yifan Tang, Wenhui Wang, Ru Zhang, Jianyi Liu, and Donglin Wang. Vla-adapter: An effective paradigm for tiny-scale vision-language-action model. *arXiv* preprint arXiv:2509.09372, 2025.
 - Zheng Wu, Wenzhao Lian, Vaibhav Unhelkar, Masayoshi Tomizuka, and Stefan Schaal. Learning dense rewards for contact-rich manipulation tasks. In 2021 IEEE International Conference on Robotics and Automation (ICRA), pp. 6214–6221. IEEE, 2021.
 - Charles Xu, Qiyang Li, Jianlan Luo, and Sergey Levine. Rldg: Robotic generalist policy distillation via reinforcement learning, 2024. URL https://arxiv.org/abs/2412.09858.
 - An Yang, Anfeng Li, Baosong Yang, Beichen Zhang, Binyuan Hui, Bo Zheng, Bowen Yu, Chang Gao, Chengen Huang, Chenxu Lv, et al. Qwen3 technical report. *arXiv preprint arXiv:2505.09388*, 2025.
 - Qiying Yu, Zheng Zhang, Ruofei Zhu, Yufeng Yuan, Xiaochen Zuo, Yu Yue, Tiantian Fan, Gaohong Liu, Lingjun Liu, Xin Liu, et al. Dapo: An open-source llm reinforcement learning system at scale. *arXiv preprint arXiv:2503.14476*, 2025.

- Zhecheng Yuan, Tianming Wei, Shuiqi Cheng, Gu Zhang, Yuanpei Chen, and Huazhe Xu. Learning to manipulate anywhere: A visual generalizable framework for reinforcement learning. *arXiv* preprint arXiv:2407.15815, 2024.
- Michał Zawalski, William Chen, Karl Pertsch, Oier Mees, Chelsea Finn, and Sergey Levine. Robotic control via embodied chain-of-thought reasoning. *arXiv preprint arXiv:2407.08693*, 2024.
- Yanjie Ze, Gu Zhang, Kangning Zhang, Chenyuan Hu, Muhan Wang, and Huazhe Xu. 3d diffusion policy: Generalizable visuomotor policy learning via simple 3d representations. *arXiv* preprint *arXiv*:2403.03954, 2024.
- Weihao Zeng, Yuzhen Huang, Qian Liu, Wei Liu, Keqing He, Zejun Ma, and Junxian He. Simplerlzoo: Investigating and taming zero reinforcement learning for open base models in the wild. *arXiv* preprint arXiv:2503.18892, 2025.
- Hongyin Zhang, Zifeng Zhuang, Han Zhao, Pengxiang Ding, Hongchao Lu, and Donglin Wang. Reinbot: Amplifying robot visual-language manipulation with reinforcement learning. *arXiv* preprint arXiv:2505.07395, 2025.
- Zijian Zhang, Kaiyuan Zheng, Zhaorun Chen, Joel Jang, Yi Li, Siwei Han, Chaoqi Wang, Mingyu Ding, Dieter Fox, and Huaxiu Yao. Grape: Generalizing robot policy via preference alignment. *arXiv preprint arXiv:2411.19309*, 2024.
- Yifan Zhong, Fengshuo Bai, Shaofei Cai, Xuchuan Huang, Zhang Chen, Xiaowei Zhang, Yuanfei Wang, Shaoyang Guo, Tianrui Guan, Ka Nam Lui, et al. A survey on vision-language-action models: An action tokenization perspective. *arXiv preprint arXiv*:2507.01925, 2025.
- Zhiyuan Zhou, Andy Peng, Qiyang Li, Sergey Levine, and Aviral Kumar. Efficient online reinforcement learning fine-tuning need not retain offline data. *arXiv preprint arXiv:2412.07762*, 2025.
- Yuxin Zuo, Kaiyan Zhang, Li Sheng, Shang Qu, Ganqu Cui, Xuekai Zhu, Haozhan Li, Yuchen Zhang, Xinwei Long, Ermo Hua, et al. Ttrl: Test-time reinforcement learning. arXiv preprint arXiv:2504.16084, 2025.

A RELATED WORKS

A.1 REINFORCEMENT LEARNING FOR LARGE LANGUAGE MODELS

Reinforcement Learning (RL) for Large Language Models (LLMs) has achieved remarkable success, demonstrating its ability to induce complex reasoning behaviors such as self-verification and iterative optimization, thereby significantly enhancing model performance on reasoning tasks (Guo et al., 2025a; Jaech et al., 2024; Liu et al., 2025c; Cui et al., 2025a; Zeng et al., 2025; Zuo et al., 2025). Recent advancements in Large Reasoning Models (LRMs), such as DeepSeek-R1 (Guo et al., 2025a), highlight the effectiveness of RL in boosting reasoning capabilities even with simple rule-based rewards, as exemplified by GRPO (Shao et al., 2024). This approach differs substantially from Reinforcement Learning from Human Feedback (RLHF) (Ouyang et al., 2022), which aligns base models with human preferences using algorithms like Proximal Policy Optimization (PPO) (Schulman et al., 2017a) and heavily relies on preference modeling.

Recent studies have increasingly focused on enhancing exploration in reinforcement learning to enable longer training horizons and improved performance. DAPO (Yu et al., 2025) introduces Clip-Higher, a decoupled variant of PPO clipping, which sets a higher upper bound relative to the lower one (e.g., $\varepsilon_L=0.2$, $\varepsilon_H=0.28$). This adjustment allows low-likelihood but potentially valuable tokens to increase in probability, thereby encouraging exploration. Building on this, POLARIS (An et al., 2025) employs a staged curriculum of temperature increases (e.g., $0.7 \rightarrow 1.0 \rightarrow 1.1$ for a 7B model) to gradually expand trajectory diversity and facilitate more robust policy discovery. In parallel, Entropy Mechanism (Cui et al., 2025b) addresses entropy collapse, a persistent issue in extended training, through methods such as Clip-Cov and KL-Cov, which selectively clip probabilities or penalize high-covariance tokens to sustain effective exploration. Similarly, ProRL (Liu et al., 2025b) combines KL control with reference policy resetting to preserve stability and extend training without degrading performance. A complementary line of work regulates entropy via temperature

tuning. Acereason-nemotron 1.1 (Liu et al., 2025d) advocates adjusting temperatures to stabilize post-scaling entropy around a target (e.g., 0.3), balancing exploration and exploitation. Liao et al. (2025) further proposes a dynamic scheduler that adapts temperature over time to maintain stable entropy, thereby supporting sustained performance gains.

A.2 VISION LANGUAGE ACTION MODELS

810

811

812

813

814 815

816

817

818

819

820

821

822

823

824

825

826

827

828

829

830

831

832

833

834

835

836

837

838

839

840

841

842

843

844

845

846

847

849

850

851

852

853 854

855 856

858

859 860

861 862

In the field of robotic manipulation tasks, VLA models (Kim et al., 2024; 2025; Liu et al., 2024; Bu et al., 2025b; Hung et al., 2025; Black et al., 2024; Pertsch et al., 2025; Intelligence et al., 2025) have shown better performance and task generalization compared to traditional policy-based approaches (Ma et al., 2022; Yuan et al., 2024). These models integrate the VLM or LLM backbone with action modules through unified end-to-end training (Zhong et al., 2025). This approach enables comprehensive multimodal understanding and fine-grained motor control (Firoozi et al., 2025). Currently, many studies are focused on enhancing the effectiveness of VLA models. For example, E-COT (Zawalski et al., 2024; Chen et al., 2025b) introduced Embedded Chain of Thought (ECoT) to improve the spatial reasoning ability of VLA models. RDT-1B and VPP (Liu et al., 2024; Hu et al., 2024) proposed diffusion-based frameworks for VLA models. Agibot world and Roboverse (Geng et al., 2025; Bu et al., 2025a) aim to build larger-scale simulation environments and trajectory datasets to improve the sim-to-real transfer and generalization capabilities of VLA models. Additionally, Dexmimicgen (Jiang et al., 2024) explores automated methods to generate high-quality trajectory data to address the issue of data scarcity in robotics. Despite the rapid advancements in the VLA domain, imitation learning remains the dominant training paradigm for VLA models (Sapkota et al., 2025; Kim et al., 2024; 2025; Liu et al., 2024; Bu et al., 2025b; Hung et al., 2025; Black et al., 2024; Pertsch et al., 2025; Intelligence et al., 2025). Current VLA models typically follow a two-stage paradigm: pretraining on multimodal data (e.g., Open X-Embodiment (O'Neill et al., 2024)) followed by SFT on collected robot trajectories. However, imitation learning is limited by its dependence on expensive, high-quality trajectory data and poor generalization to unseen scenarios.

Recently, some efforts have attempted to apply RL to VLA training. VLA RL Methods GRAPE (Zhang et al., 2024) utilized Direct Preference Optimization (DPO) (Rafailov et al., 2023) to train VLA models by integrating human preferences. ConRFT (Chen et al., 2025c) introduced Reinforced Fine-Tuning (Trung et al., 2024) to train VLA models in real-world environments, iteratively training VLAs through alternating RL and SFT rounds. ReinboT (Zhang et al., 2025) focused on dense reward design and optimized VLA models through reward maximization. Guo et al. (2025b) proposed an iterative training framework that combines Supervised Fine-Tuning (SFT) and RL stages to address training instability and computational overhead. More recent works have further advanced VLA RL methods. Concurrently, RIPT-VLA (Tan et al., 2025) investigates a closely related problem, employing RLOO (Ahmadian et al., 2024) for VLA RL training. Moreover, Liu et al. (2025a) investigates RL's impact on VLA generalization capabilities, demonstrating significant improvements over SFT in unseen environments, objects, and textures. RLinf (Team, 2025) designed a flexible, scalable framework for VLA RL that unifies rendering, inference, and training, improving both VLA training efficiency and performance. VLA-RL (Lu et al., 2025) applies the PPO algorithm to the VLA model. TGRPO (Chen et al., 2025d) uses Claude3.7 to evaluate trajectories and optimizes VLA with GRPO. RFTF (Shu et al., 2025) uses value models to generate dense rewards in embodied scenarios for VLA online RL. Compared to the above works, our paper further explores the effectiveness of VLA RL on real-world robotic tasks. We also conduct comprehensive analyses on how VLA RL addresses data scarcity challenges and improves policy generalization.

B PRELIMINARIES

To provide an intuitive illustration of the existing gap when extending RL methodologies from LLMs to the VLA domain, we formalize RL for both LLMs and VLA models, presenting their state representations, action spaces, reward functions, and environments in this section.

B.1 RL FORMULATION FOR LLMS

State (s_t) : At step t, the state s_t comprises the input prompt and previously generated tokens:

$$s_t = (x_{\text{prompt}}, y_1, y_2, \dots, y_{t-1}),$$
 (5)

where x_{prompt} denotes the initial prompt and y_t denotes the t-th generated token.

Action (a_t) : An action corresponds to selecting the next token from the vocabulary \mathcal{V} . At each step, the policy outputs a probability distribution over tokens, and the action token is selected via random sampling. Formally, the action is defined as:

$$a_t = y_t \in \mathcal{V}, \quad \text{where} \quad y_t \sim \pi_\theta(\cdot | s_t) = \operatorname{softmax} (f_\theta(s_t)/T),$$
 (6)

where $f_{\theta}(s_t) \in \mathbb{R}^{|\mathcal{V}|}$ represents the LLM logit outputs and T is the temperature parameter controlling the randomness of sampling.

Environment: The environment provides reward signals upon sequence completion. In rule-based settings, binary rewards are assigned based on the correctness. Alternatively, learned reward models or human feedback systems provide continuous rewards based on criteria such as helpfulness, harmlessness, or task alignment. The reward is computed as follows:

$$r(\tau) = \begin{cases} 1, & \text{if } \tau \text{ satisfies correctness criteria} \\ 0, & \text{otherwise} \end{cases}, \quad \text{or} \quad r(\tau) = R_{\phi}(\tau) \in [0, 1], \tag{7}$$

where R_{ϕ} is a learned reward model and $\tau=(x_{\text{prompt}},y_1,y_2,\ldots,y_{T_{\text{seq}}})$ represents the complete generated sequence of length T_{seq} .

Rollout: Given an input prompt x_{prompt} , the LLM auto-regressively generates a sequence by sampling tokens from $\pi_{\theta}(y_t|s_t)$ until termination, without intermediate environmental feedback. With a non-zero temperature T, the policy can produce diverse rollouts that explore different solution paths.

B.2 RL FORMULATION FOR VLAS

State (s_t) : The state consists of multimodal observations including visual input (RGB images, depth maps, or point clouds), proprioceptive information (joint angles, end-effector pose), and language instructions of the tasks. Formally, the state is defined as:

$$s_t = (o_t^{\text{vis}}, o_t^{\text{prop}}, l_{\text{task}}), \tag{8}$$

where o_t^{vis} is multimodal observations, o_t^{prop} is proprioceptive information, and l_{task} is language instructions.

Action (a_t) : Actions are control commands in the robot action space, typically end-effector deltas or joint angle targets, where $a_t \in \mathbb{R}^d$ (e.g., d=7 for 6-DoF pose plus gripper position). Most VLA policies generate actions through either a diffusion-based action expert or a discrete action tokenizer. The action is defined as follows:

$$a_t = Decoder(h_{\theta}(s_t)), \quad Decoder \in \{\text{Diffusion Expert, Action Tokenizer}\}, \quad a_t \in \mathbb{R}^d, \quad (9)$$

where $h_{\theta}(s_t)$ represents the hidden state of s_t in the VLA model, and Decoder is the action decoder.

Environment: The environment represents the physical world or simulation where the robot operates. It provides state transitions $s_{t+1} = \text{Env}(s_t, a_t)$ and reward signals:

$$r_t = \alpha \cdot I_{\text{success}} + (1 - \alpha) \cdot \sum_i w_i \cdot \phi_i(s_t, a_t), \quad \alpha \in [0, 1], \quad I_{\text{success}} = \begin{cases} 1, & \text{if task success} \\ 0, & \text{otherwise} \end{cases}, (10)$$

where $\phi_i(s_t, a_t)$ represents process rewards (e.g. distance to goal), w_i are weights, and α balances outcome and process rewards.

Rollout: VLA models generate trajectories through iterative interaction with the environment. At each timestep, the policy π_{θ} takes the current state s_t as input and outputs an action chunk $(a_t, a_{t+1}, \ldots, a_{t+k-1})$ of length k. The robot executes these actions sequentially and the environment produces updated states based on physical dynamics. After execution, the model takes the new state s_{t+k} as input and generates the next action chunk. This process continues until task completion or maximum episode length, producing a complete trajectory $\tau = ((s_0, a_0), (s_1, a_1), \ldots, (s_T, a_T))$ through interactive sampling.

B.3 GROUP RELATIVE POLICY OPTIMIZATION

Group Relative Policy Optimization (GRPO) (Shao et al., 2024) is an RL method that eliminates the value function by computing advantages through group-relative normalization. Given an initial state s_0 , the behavior policy $\pi_{\theta_{\text{old}}}$ generates G trajectories $\{\tau_i\}_{i=1}^G$. The GRPO objective employs PPO-style clipping with KL regularization to constrain policy updates:

$$J_{\text{GRPO}}(\theta) = \mathbb{E}_{s_0 \sim \mathcal{D}, \{\tau_i\} \sim \pi_{\theta_{\text{old}}}} \left[\frac{1}{G} \sum_{i=1}^{G} \frac{1}{|\tau_i|} \sum_{t=1}^{|\tau_i|} \min \left(r_{i,t}(\theta) \hat{A}_i, \text{clip}(r_{i,t}(\theta), 1 - \epsilon, 1 + \epsilon) \hat{A}_i \right) - \beta D_{\text{KL}}(\pi_{\theta} || \pi_{\text{ref}}) \right],$$

$$(11)$$

where the importance sampling ratio $r_{i,t}(\theta)$ and the normalized advantage \hat{A}_i are defined as:

$$r_{i,t}(\theta) = \frac{\pi_{\theta}(a_{i,t}|s_{i,t})}{\pi_{\theta_{\text{old}}}(a_{i,t}|s_{i,t})}, \quad \hat{A}_i = \frac{R_i - \text{mean}(\{R_i\}_{i=1}^G)}{\text{std}(\{R_i\}_{i=1}^G)}.$$
 (12)

Here R_i denotes the total reward of the *i*-th trajectory, $\epsilon > 0$ is the PPO clipping parameter that limits the policy ratio, and $\beta > 0$ is the coefficient controlling the strength of KL regularization with respect to the reference policy $\pi_{\rm ref}$.

C FAILURE MODES OF SIMPLEVLA-RL

Table 6: Impact of initial model capability on **SimpleVLA-RL** performance.

	RoboTwin2.0						
	Move Can Pot	Place A2B Left	Place A2B Right	Place Phone Stand	Pick Dual Bottles	Avg	
0 trajs SFT	0	0	0	0	0	0	
+ŘL	0	0	0	0	0	0	
100 trajs SFT	9.4	7.8	7.8	10.1	1.2	7.3	
+RL	51.6	25.0	27.2	18.8	4.3	25.4	
Δ	+42.2	+17.2	+19.4	+8.7	+3.1	+18.1	
1000 trajs SFT	28.1	37.5	28.7	17.1	29.7	28.2	
+RL	61.2	45.3	37.5	39.6	68.3	50.4	
Δ	+33.1	+7.8	+8.8	+22.5	+38.6	+22.2	

This subsection investigates the failure conditions of **SimpleVLA-RL** and key influencing factors. Through experiments on five RoboTwin2.0 tasks, we find that the model priors are the critical factor determining RL effectiveness.

Settings Each task is trained under domain randomization with a single-task setting. We compare three model variants: (1) the OpenVLA-OFT base model without trajectory fine-tuning (0 trajectories SFT); (2) the model fine-tuned with 100 demonstration trajectories per task (100 trajectories SFT); and (3) the model fine-tuned with 1000 demonstration trajectories per task (1000 trajectories SFT). All models undergo **SimpleVLA-RL** training on 1000 training scenarios and are evaluated on 100 held-out test scenarios.

RL fails completely when the base model has no initial task ability. Table 6 reports the results. The base model (0-trajectory SFT) achieves a 0% success rate across all tasks, exhibiting no task-relevant behaviors. Despite extensive pretraining, OpenVLA shows extremely limited zero-shot generalization, consistent with findings in Kim et al. (2025). Because no successful trajectories are generated during sampling and only outcome rewards (without process rewards) are employed, every trajectory receives zero reward. As a result, RL is unable to improve performance, which remains at 0%.

The model prior has a significant impact on the effectiveness of RL. Initial capability is strongly correlated with post-RL performance. The 100-trajectory SFT model improves from 7.3% to 25.4% (an 18.1% gain), while the 1000-trajectory SFT model improves from 28.2% to 50.4% (a 22.2% gain) in average success rate. This trend is consistent across tasks. For instance, in the *move can*

pot task, the 100-trajectory SFT model improves from 9.4% to 51.6%, whereas the 1000-trajectory SFT model improves from 28.1% to 61.2%. These results highlight that stronger initial capabilities provide more effective starting points for exploration, thereby facilitating greater performance improvements.

RL effectiveness has a threshold: when initial ability is too low, improvements remain negligible. Our findings further reveal that the effectiveness of RL is subject to a performance threshold. When initial success rates are very low, online RL with outcome rewards yields only marginal improvements. For example, in the *pick dual bottles* task, the 100-trajectory SFT model improves from 1.2% to 4.3%, while the 1000-trajectory SFT model improves from 29.7% to 68.3%. Similarly, in the *place phone* task, the 100-trajectory SFT model gains 8.7%, compared to a 22.5% gain for the 1000-trajectory SFT model. The results indicate that a minimal level of task competence is essential for effective RL. Below this threshold, exploration is ineffective and RL fails to produce meaningful gains.

D MULTI-TASK RL TRAINING ON LIBERO-90

To evaluate the effectiveness of **SimpleVLA-RL** in multi-task mixed training settings, we conduct RL training on the LIBERO-90 task suite, which contains 90 different tasks. Each task consists of 50 scenarios, resulting in a total of 4,500 scenarios across all 90 tasks that serve as the training set for **SimpleVLA-RL**. Figure 6 shows the results of different models on LIBERO-90, as well as the performance of OpenVLA-OFT SFT and OpenVLA-OFT RL on LIBERO-90 under the one-trajectory SFT setting.

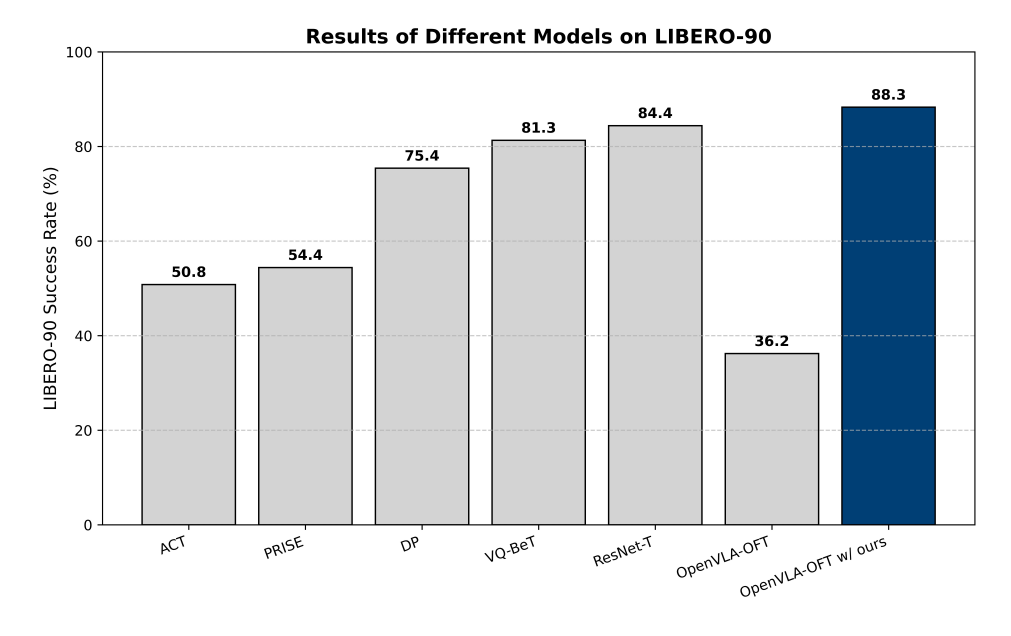


Figure 6: Results of different models on LIBERO-90.

E COMPARISON OF LLM AND VLA ROLLOUT ALGORITHMS

To better illustrate the concrete rollout process in **SimpleVLA-RL** and highlight the key differences between VLA rollout in **SimpleVLA-RL** and LLM rollout in the veRL framework, we present a comparative pseudo-code implementation in Listing 1.

```
1026
        def rollout(policy, dataset, number_sample=8, max_steps=None):
1027
          rollout_dataset = []
1028
          for batch in dataset:
1029
             batch = batch.repeat(number_sample)
1030
             # LLM generates diverse outputs using random sampling
1031
             outputs = policy.generate(batch, temperature=1.0)
1032
             rollout_dataset.append((batch, outputs))
1033
             # Parallel env initialization and interaction
             envs = env_process_pool.submit(batch.initialize)
1034
             states = env_process_pool.submit(envs.setup)
1035
             for t in range(max_steps):
1036
                # VLA generates diverse trajectories using temperature
1037
            sampling on action tokens
1038
                actions = policy.generate(states, temperature=1.0)
                rollout_dataset.append({f"{e.name}_step_{t}": (s,a)} for e,s,a
1039
            in zip(envs, states, actions) })
1040
                states, dones = env_process_pool.submit(envs.step, actions)
                # Remove completed tasks
1042
                active = [(e,s) for e,s,d in zip(envs,states,dones) if not d]
1043
                if not active:
                   break
1044
                envs, states = zip(*active)
1045
          return rollout_dataset
1046
1047
```

Listing 1: Pseudo-code for the adopted veRL rollout function: from LLM-based generation to interactive VLA sampling with synchronous environment parallelism.

Table 7: RoboTwin 2.0 task classification based on planning horizon and required steps.

Task Name	Steps	Horizon	Horizon Group			
Short H	Iorizon '	Tasks (112-13	0 steps)			
lift_pot	112	Short				
beat_block_hammer	113	Short	Average: 121 steps			
pick_dual_bottles	127	Short	Count: 4 tasks			
place_phone_stand	130	Short				
Medium Horizon Tasks (151-223 steps)						
move_can_pot	151	Medium				
place_a2b_left	155	Medium	Average: 176 steps			
place_empty_cup	174	Medium	Count: 4 tasks			
handover_mic	223	Medium				
Long H	Iorizon T	Tasks (283-313	3 steps)			
handover_block	283	Long	Average: 298 steps			
stack_bowls_two	313	Long	Count: 2 tasks			
Extra Long Horizon Tasks (466-637 steps)						
blocks_rank_rgb	466	Extra-Long	Average: 552 steps			
put_bottles_dustbin	637	Extra-Long	Count: 2 tasks			
Overall Statistics Total: 12 tasks, Average: 256 steps						

F EXPERIMENTAL CONFIGURATION AND IMPLEMENTATION

F.1 ROBOTWIN2.0 TASK CLASSIFICATION AND DETAILS

We classified the 12 tasks in RoboTwin2.0 based on their average number of steps, categorizing them into Short Horizon Tasks, Medium Horizon Tasks, Long Horizon Tasks, and Extra Long Horizon Tasks. The Table7 shows the specific number of steps and classification for each task.

Detailed descriptions of the 4 real-world tasks (Stack Bowls, Handover Block, Pick Bottle, and Click Bell) and 12 RoboTwin2.0 tasks can be found at https://robotwin-platform.github.io/doc/tasks/index.html.

F.2 BACKBONE MODIFICATION DETAILS

Our implementation of the OpenVLA-OFT model differs from the official version. To achieve improved training and inference efficiency, we utilize only single-view images, language instructions, and robot proprioceptive states as model inputs, whereas the official model additionally incorporates wrist camera images. Additionally, in the LIBERO, we don't use robot proprioceptive states in model inputs. Regarding the model architecture, we employ only parallel decoding and action chunking designs. We use the LLaMA2 output head to generate action tokens and the cross-entropy loss, whereas the official model uses an MLP to generate continuous actions and L1 regression. Due to the differences in model inputs and architecture, we cannot use the official checkpoints. We modify the official codebase and performed SFT from scratch using the same datasets and hyperparameters as the official implementation.

F.3 IMPLEMENTATION DETAILS AND HYPERPARAMETERS

For training infrastructure, we employ $8\times NVIDIA$ A800 80GB for full-parameter training. The training hyperparameters are configured as follows: learning rate $lr=5\times 10^{-6}$, training batch size of 64, sampling count of 8, mini-batch size of 128, clip ratio $\varepsilon_L=0.2$, $\varepsilon_H=0.28$, and temperature T=1.6. The number of action chunks is 8 in the LIBERO and 25 in the RoboTwin1.0&2.0. The model is configured with a total of 256 action tokens. The maximum environment interaction step is set to 512 in the LIBERO and 200, 400, or 800 in the RoboTwin1.0&2.0, depending on different tasks. During the rollout phase of RL training, we employ random sampling. For evaluation, we utilize greedy sampling, with each benchmark tested three times for reproducibility.

F.4 ROBOT HARDWARE DETAILS

For real-world experiments, we employ an AgileX Cobot Magic, which is a mobile platform with an Aloha configuration consisting of four robotic arms. Each arm is an AgileX Piper with six degrees of freedom, equipped with a one-DoF parallel gripper. A RealSense D435 RGB-D camera is mounted on the platform, capturing RGB images in real time at a resolution of 640×480 with a frame rate of approximately 30 Hz.

G THE USE OF LARGE LANGUAGE MODELS

We utilized LLMs for grammatical refinement and clarity improvements in our manuscript. Specifically, we used ChatGPT (GPT-5-Thinking) to help polish the language and correct grammatical errors in our draft. The assistance was limited to improving readability and ensuring adherence to academic writing conventions, while all technical content, experimental design, and scientific contributions remain entirely our own work.